AAEC/E478

AAEC/E478


# AUSTRALIAN ATOMIC ENERGY COMMISSION

## RESEARCH ESTABLISHMENT

## LUCAS HEIGHTS

# THE FAILURE OF CIRCUMFERENTIALLY FLAWED STAINLESS STEEL TUBES UNDER BENDING STRESSES

by

P.M. KELLY
B. ZYBENKO

November 1979

ISBN 0 642 59677 8

AUSTRALIAN ATOMIC ENERGY COMMISSION
RESEARCH ESTABLISHMENT
LUCAS HEIGHTS

# THE FAILURE OF CIRCUMFERENTIALLY FLAWED STAINLESS STEEL TUBES UNDER BENDING STRESSES

P.M. KELLY
B. ZYBENKO

## ABSTRACT

The failure of circumferentially flawed, 100 mm diameter type 321 stainless steel tubes under bending stresses was examined experimentally. Both through-wall and partial thickness flaws were tested. The results were in good agreement with the predictions of a net section plastic collapse model.

National Library of Australia card number and ISBN 0 642 59677 8

The following descriptors have been selected from the INIS Thesaurus to describe the subject content of this report for information retrieval purposes. For further details please refer to IAEA-INIS-12 (INIS: Manual for Indexing) and IAEA-INIS-13 (INIS: Thesaurus) published in Vienna by the International Atomic Energy Agency.

STRESSES; STRESS ANALYSIS; STAINLESS STEEL-321; FAILURES; PIPES; CRACKS; BENDING; FLEXURAL STRENGTH

CONTENTS

## 1. INTRODUCTION

This project was undertaken to provide an experimental test of the results of a theoretical analysis of the failure of circumferentially flawed stainless steel tubes under bending stress. The theoretical treatment of failure prediction was developed for the Electric Power Research Institute (EPRI) by Kanninen et al. [1976] and verified for a 100 mm diameter x 8 mm wall thickness pipe. It has been extended to the case of thinner type 321 stainless steel tubing used in the cooling circuit of the materials testing reactor HIFAR.

This analysis is essentially based on a net section plastic collapse criterion and can be applied to tubes subjected to a bending load either with or without internal pressure. As the coolant pressure in HIFAR is only 300 kPa (44 psi), the effects of this internal pressure can usually be neglected, and, with a few exceptions, the experimental tests were conducted with no internal pressure.

## 2. THEORETICAL ANALYSIS

The parameters used by Kanninen et al. [1976] to analyse the failure of a flawed pipe containing a through-wall flaw are shown in Figure 1. The pipe is assumed to contain a flaw that subtends an angle $2\alpha$ at the centre of the pipe. The load acting on the pipe is a bending moment $M_b$. The neutral axis, where the stress reverses sign, subtends an angle $2\beta$ at the centre of the pipe and $\beta$ is given by:

$$\beta = \frac{\pi-\alpha}{2} \tag{1}$$

By taking moments about the centre plane of the pipe BB', the value of $M_b$ can be determined from:

$$M_b = 2\sigma R^2 t\,(2\sin\beta - \sin\alpha) \tag{2}$$

The conditions for failure can be calculated from Equation 2 by replacing $\sigma$ (the stress acting in front of the flaw tip) with the failure stress $\sigma_f$. Similarly, the lower bending moment corresponding to the initiation of slow flaw growth is given by Equation 2 with $\sigma=\sigma_i$. Both of these conditions are, therefore, related to the situation where the net stress in the remaining unflawed section of pipe reaches some critical value - a net section plastic collapse criterion.

The failure stress $\sigma_f$ and a failure initiation stress $\sigma_i$ are given by the empirical relation:

$$\sigma_f = \frac{\sigma_y + \sigma_u}{2} \tag{3}$$

and

$$\sigma_i = \frac{\sigma_f + \sigma_y}{2} = 0.75\sigma_f \tag{4}$$

where $\sigma_y$ is the 0.2 per cent proof stress of the material (241 MPa in this case) and $\sigma_u$ is the ultimate tensile strength (UTS; 600 MPa). Using these values in Equations 3 and 4 gives $\sigma_f$ = 421 MPa and $\sigma_i$ = 316 MPa. Theoretical through-thickness flaw failure criteria were calculated and are compared with the experimental results in Figure 2. Note that Figure 2 is plotted in terms of $M_b/\sigma_f Rt^2$ so that at $\alpha$ = 0 the <u>failure</u> criterion ($\sigma_f$) corresponds to $M_b/\sigma_f Rt^2 = 4$ whereas the <u>failure initiation</u> criterion ($\sigma_i$) corresponds to $M_b/\sigma_f Rt^2 = 3$.

The case of partial-thickness flaws was also treated by Kanninen et al. Their approach was an empirical one, where a flaw of depth ($a < t$) subtending an angle $2\alpha$ was taken to be equivalent to a through-thickness flaw of angle $(a/t)2\alpha$, i.e. a through-thickness flaw of equivalent area to the partial thickness flaw. In addition, the failure mechanism was considered to be that of slow flaw growth through the wall at stress $\sigma_i$, eventually resulting in a through-thickness flaw which would fail at $\sigma_f$. Note the use of the lower stress $\sigma_i$ (rather than $\sigma_f$) as the failure condition. This was done to give a version of the 'leak-before-break' criterion, where a partial thickness defect could grow through the wall at a stress below that required for failure of the corresponding full thickness flaw. If the failure stress had been taken to be

$\sigma_f$, then no partial thickness defect could 'leak-before-break' merely because (a/t) must always be less than unity.

The relevant partial thickness equivalents of Equations 1 and 2 fall into two categories. First, there is the situation in which $\beta_L$ (the value of $\beta$ for the partial thickness case) is less than $(\pi-\alpha)$, and the second is the case in which $\beta_L > (\pi-\alpha)$. The equations for each case are as follows:

Case (i)

$$\beta_L < (\pi-\alpha)$$

$$\beta_L = \frac{\pi-x\alpha}{2} \tag{5}$$

$$M_L = 2\sigma_i R^2 t[2\sin\beta_L - x \sin\alpha] \tag{6}$$

where x = a/t, and

Case (ii)

$$\beta_L > (\pi-\alpha)$$

$$\beta_L = \pi + \frac{1}{1-x}\left(\frac{x\ \alpha-\pi}{2}\right) \tag{7}$$

$$M_L = 2\sigma_i R^2 t[2(1-x)\ \sin\beta_L + x \sin\alpha] \tag{8}$$

The partial thickness failure criteria calculated from Equations 5 to 8 are shown as dot-dash lines in Figure 3. As was the case in Figure 2, the intercept of 3 at $\alpha = 0$ corresponds to a failure initiation criterion ($\sigma_i$).

## 3. EXPERIMENTAL

The HIFAR coolant pipework consists of 102 mm diameter stainless steel tubing of 3.17 mm wall thickness, but as such tubing was not readily available, the experiments were conducted on tubes of the same outside diameter and a smaller wall thickness (2.23 mm). The tubes were of AISI 321 specification (0.08% C; 1.0% Si; 2.0% Mn; 17-19% Cr; 9-12% Ni;

0.4% min. Ti) with a 0.2 per cent proof stress of 241 MPa, a UTS of 600 MPa and an elongation of 55 per cent. The tubes were cut into 750 mm lengths and a circumferential flaw was cut at the middle of each tube. For through-wall flaws, the parameters were as shown in Figure 1. The length of the hacksaw cut flaw was varied to give different values of the subtended angle $2\alpha$, and the tips of each were sharpened with a jeweller's file to give a sharp notch.

Partial thickness flaws were introduced by milling a groove circumferentially round part of the tube. The depths of the grooves were between 50 and 90 per cent of the wall thickness and the angle subtended at the centre varied from 80 to 240°. The radius at the root of the flaw was 0.1 mm.

To allow the depth and root radius of the flaw to be measured along its full length, the depth of the partial thickness flaws was measured by a replication technique. A cast of the groove was made with Dow Corning 3120 RTV silicone rubber. After the rubber had set, the replica was peeled off and the profile measured with a travelling microscope.

Partial thickness flaws of consistent depth were difficult to obtain because of the small wall thickness and ovality of most tubes. Attempts were made to produce two series of flawed tubes, one set having 50 per cent depth flaws and the other having 75 per cent depth flaws. However, in both cases, the flaw depth varied, so that the resulting series of tubes corresponded to 50 to 69 per cent and 75 to 87 per cent.

The flawed tubes were loaded in a four-point bend jig (Figure 4) mounted in a universal testing machine. The maximum load (P) to initiate flaw propagation was read from the dial of the testing machine; the bending moment on the pipe (M) was then calculated from the equation:

$$M = \frac{P}{2} \times \ell \qquad (9)$$

where $\ell$ is the distance between the supports.

As the through-thickness flaw extended circumferentially, the applied load decreased. The propagating flaw could be halted by further reducing the applied load. This allowed the new flaw length to be measured by increasing

the load and noting the value at which flaw growth recommenced. This procedure allowed several experimental data points to be obtained from a single tube.

Because of the thin tube wall, some inaccuracies were introduced by the local crushing of the tube at the loading points (Figure 5). Further, the flawed section of the tube became progressively more oval as the test progressed, with the result that the position of the neutral axis could not be determined accurately.

## 4. RESULTS

The results for tubes with through-wall and partial thickness flaws are shown in Tables 1 and 2 respectively.

If the results for the through-thickness flaws are plotted against the predictions of the EPRI analysis (Figure 2) and $\sigma_f$ is taken as the criterion for failure, it is apparent that there is good agreement between theory and experiment. Although the data corresponding to the initial propagation of the original flaw (open circles) lie below the full curve ($\sigma_f$ criterion) and are somewhat closer to the dotted curve ($\sigma_i$ criterion), the agreement between prediction and experiment is still good. The plots of predicted and experimental values (Figure 6) confirm that the two sets of values agree to better than ± 20 per cent.

The results for the partial thickness flaws of variable depth are shown as open circles on Figure 3. The agreement with predicted values is reasonable, with the shallow flaws (open circles) giving experimental results that generally exceed theoretical predictions, and the deeper flaws (black circles) showing the opposite behaviour. This is more obvious in Figure 7.

## 5. DISCUSSION

The experimental results for through-wall and partial thickness flaws agree with the theoretical predictions to within ± 20 per cent. The agreement for partial thickness flaws is slightly worse than that for through-thickness flaws. Considering the simplicity of the theoretical net section plastic

collapse approach, this measure of agreement is good, particularly as many experimental difficulties caused by the thinness of the tube could have contributed to the lack of precision. These difficulties included:

(a) Slight ovality of the tubes. During the progress of the test the flawed sections of the tube became progressively more oval in the region of the flaw. This resulted in a shift of the neutral axis to a position that could not be estimated with accuracy.

(b) Variations in the depth of partial thickness flaws along the length of the milled cut. These variations were relatively more significant in thin walled tube.

(c) The tendency of the tube wall to crush at the loading points (see Figure 5).

An additional source of error may have been the use of published values of the mechanical properties of the steel, rather than measured values. Properties were measured on flattened sections of tubing; however, because of the work hardening introduced during specimen preparation, the results were not regarded as being reliable.

It should be noted that although the EPRI analysis has been verified for flaw growth in thin walled tubing, failure is likely to result from the mechanical bending of the tube at points of high bending moment, or by crushing at points of high load. These failure modes should not be ignored in any pipework analysis as they may make the simple EPRI analysis irrelevant.

## 6. CONCLUSIONS

Despite the simplicity of the analysis, the theoretical predictions of the net section plastic collapse criterion developed by Kanninen et al. [1976] for circumferentially flawed tubes in four-point bending are in reasonable agreement with experimental results obtained on flawed stainless steel pipes having much thinner walls than those used to verify the analysis.

## 7. REFERENCE

Kanninen, M.F., Broek, D., Marschall, C.W., Rybicki, E.F., Sampath, S.G., Simonen, F.A. and Wilkowski, G.M. [1976] - Mechanical fracture predictions for sensitised stainless steel piping with circumferential crack. EPRI NP-192.

TABLE 1

RESULTS FOR THROUGH-WALL FLAWED PIPE TESTED IN FOUR POINT BEND

| Subtended Angle $2\alpha$ (deg) | Distance Between Supports (m) | Load (N) | Experimental Moment (N m) | Experimental Dimensionless Factor $M_b/\sigma_f R^2 t$ $\sigma_f$ = 421 MPa | Predicted Dimensionless Factor $\frac{M_b}{\sigma_f R^2 t}$ |
|---|---|---|---|---|---|
| 60 | 0.165 | 71081 | 5864 | 2.50 | 2.86 |
| 77 | 0.165 | 68472 | 5649 | 2.41 | 2.53 |
| 90 | 0.165 | 61578 | 5080 | 2.16 | 2.28 |
| 92 | 0.165 | 56822 | 4688 | 2.00 | 2.24 |
| 92 | 0.160 | 56881 | 4550 | 1.94 | 2.24 |
| 92 | 0.115 | 73160 | 4206 | 1.79 | 2.24 |
| 114 | 0.115 | 74013 | 4256 | 1.81 | 1.84 |
| 115 | 0.115 | 68727 | 3952 | 1.68 | 1.82 |
| 134 | 0.170 | 33108 | 2814 | 1.20 | 1.49 |
| 136 | 0.170 | 42454 | 3609 | 1.54 | 1.46 |
| 141 | 0.115 | 57645 | 3315 | 1.41 | 1.38 |
| 164 | 0.115 | 44347 | 2550 | 1.09 | 1.04 |
| 164 | 0.170 | 26655 | 2265 | 0.965 | 1.04 |
| 182 | 0.115 | 29499 | 1696 | 0.723 | 0.804 |
| 187 | 0.115 | 27460 | 1579 | 0.673 | 0.744 |
| 196 | 0.115 | 25577 | 1470 | 0.626 | 0.644 |
| 215 | 0.115 | 18584 | 1068 | 0.455 | 0.458 |

TABLE 2

RESULTS FOR PARTIALLY FLAWED PIPE TESTED IN FOUR POINT BEND

| Subtended Angle $2\alpha$ (deg) | Depth of the Flaw a/t | Distance Between Supports (m) | Load (N) | Experimental Moment (N m) | Experimental Dimensionless Factor $M_b/\sigma_f R^2t$ $\sigma_f$ = 421 MPa | Predicted Dimensionless Factor $M_b/\sigma_f R^2t$ |
|---|---|---|---|---|---|---|
| 82 | 0.87 | 0.17 | 52152 | 4433 | 1.89 | 2.00 |
| 100 | 0.79 | 0.17 | 48367 | 4111 | 1.75 | 1.92 |
| 120 | 0.57 | 0.32 | 33872 | 5420 | 2.31 | 2.13 |
| 128 | 0.75 | 0.17 | 45905 | 3902 | 1.66 | 1.73 |
| 134 | 0.76 | 0.16 | 38776 | 3102 | 1.32 | 1.66 |
| 160 | 0.61 | 0.167 | 65754 | 5490 | 2.34 | 1.83 |
| 180 | 0.55 | 0.165 | 64724 | 5340 | 2.28 | 1.90 |
| 180 | 0.50 | 0.165 | 67078 | 5534 | 2.36 | 2.02 |
| 192 | 0.69 | 0.165 | 55270 | 4560 | 1.94 | 1.48 |
| 240 | 0.58 | 0.32 | 30489 | 4878 | 2.08 | 1.71 |

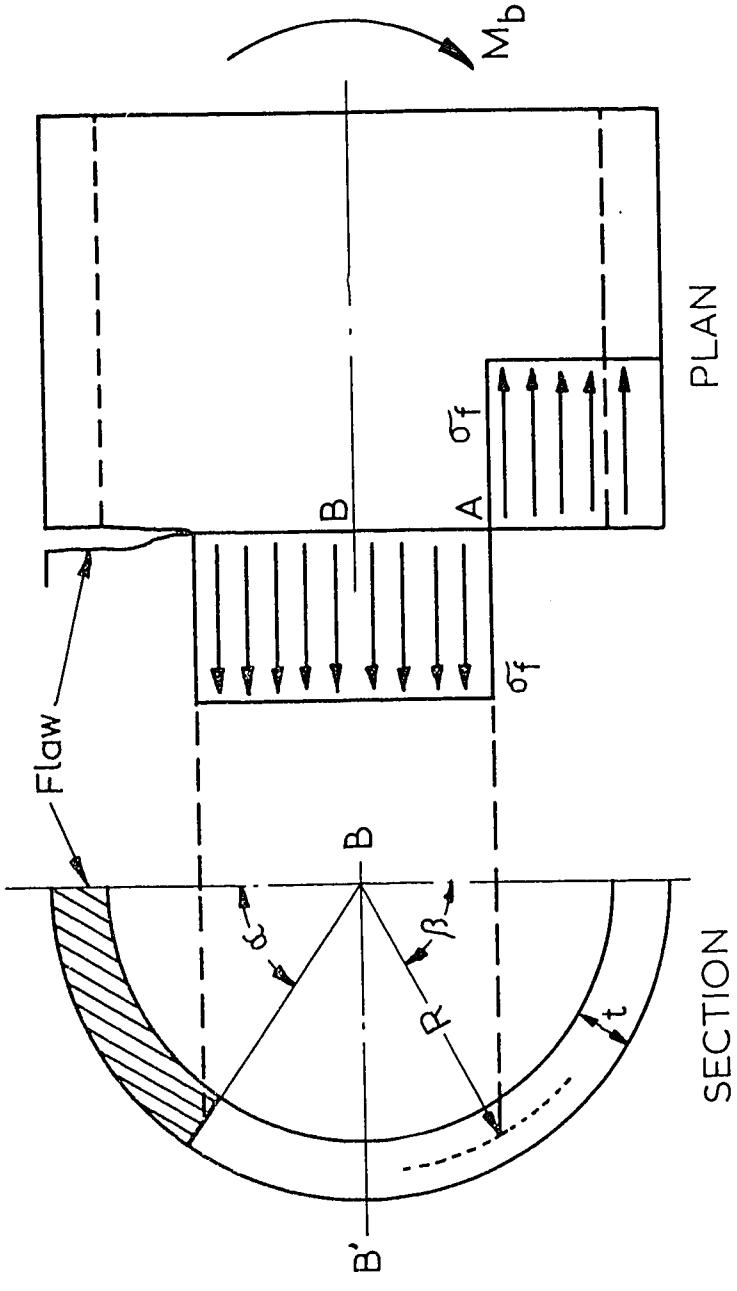


FIGURE 1. SCHEMATIC DIAGRAM SHOWING PARAMETERS USED TO DESCRIBE THE THROUGH-WALL THICKNESS FLAW

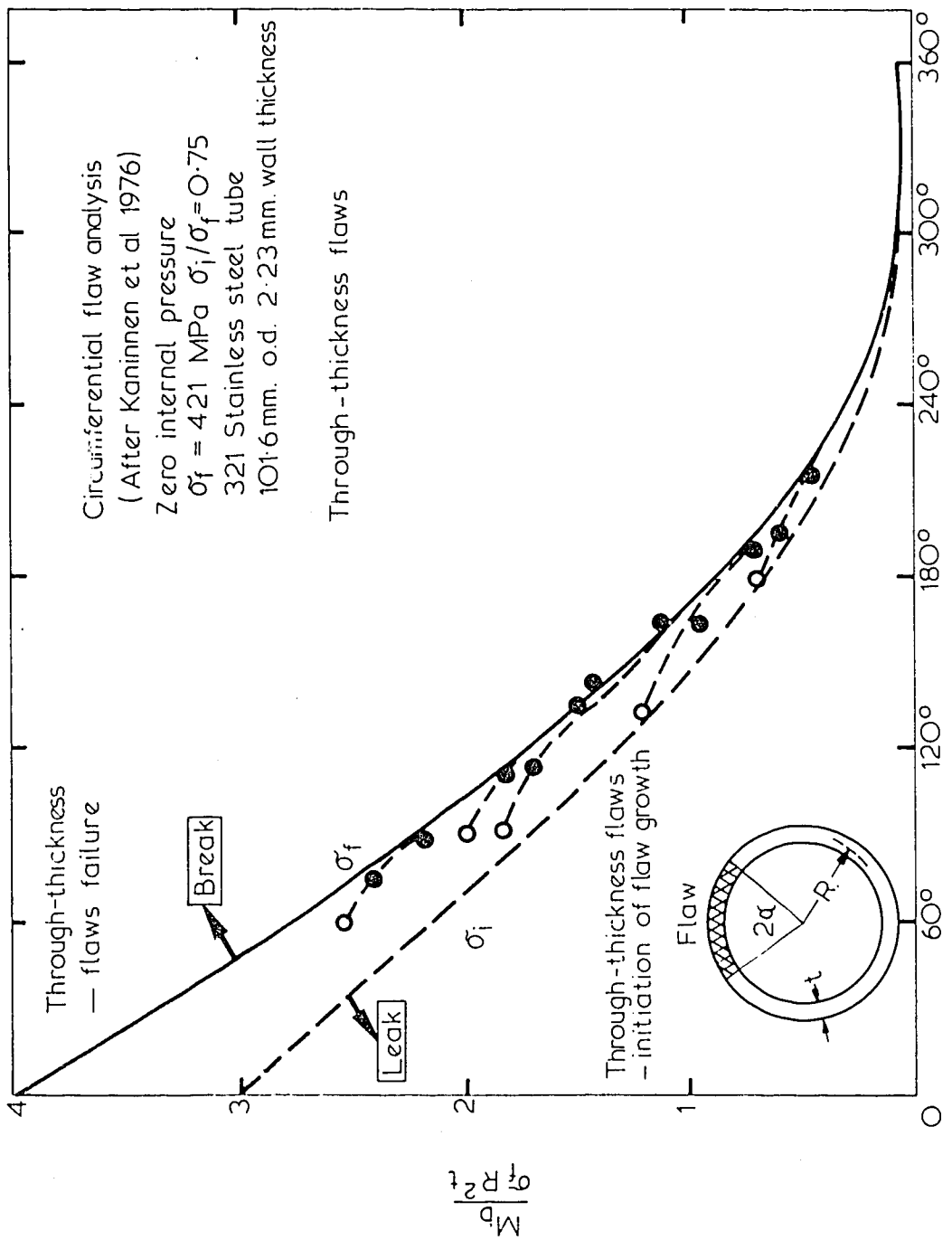


**FIGURE 2. PREDICTED AND EXPERIMENTAL RESULTS FOR THROUGH-THICKNESS FLAWS**

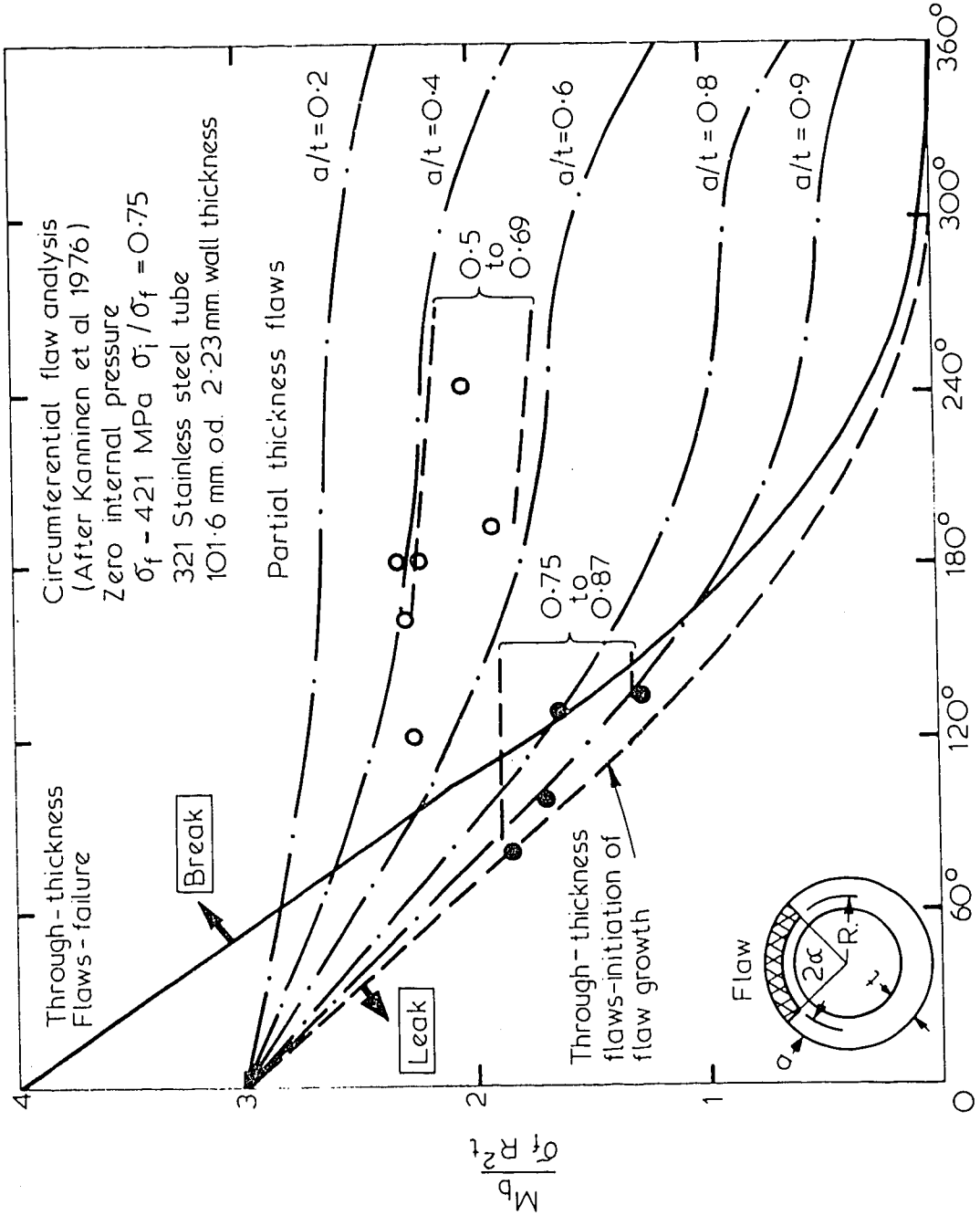


**FIGURE 3. PREDICTED RESULTS FOR THROUGH-WALL AND PARTIAL THICKNESS FLAWS. ALSO SHOWN ARE THE EXPERIMENTAL RESULTS FOR PARTIAL THICKNESS FLAWS**

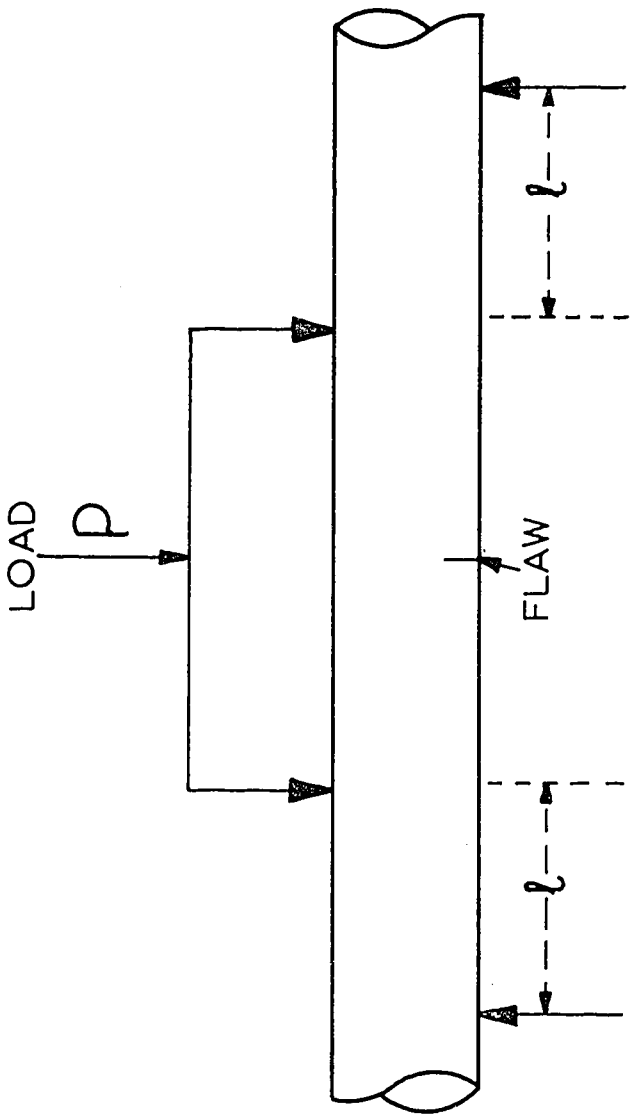


FIGURE 4. FOUR-POINT BEND TEST GEOMETRY

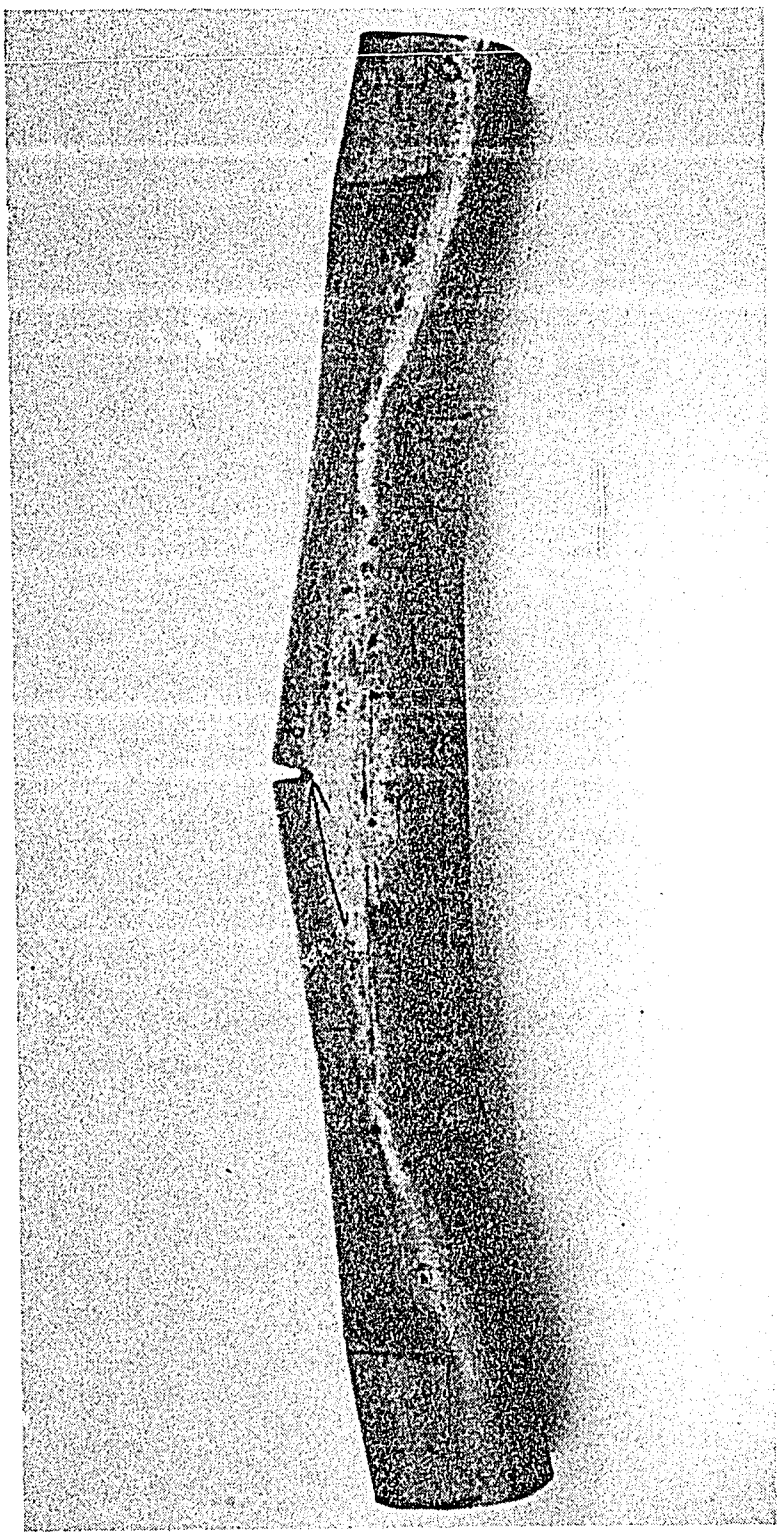

FIGURE 5. AN ILLUSTRATION OF THE TENDENCY OF THE TUBE WALL TO CRUSH AT THE LOADING POINTS

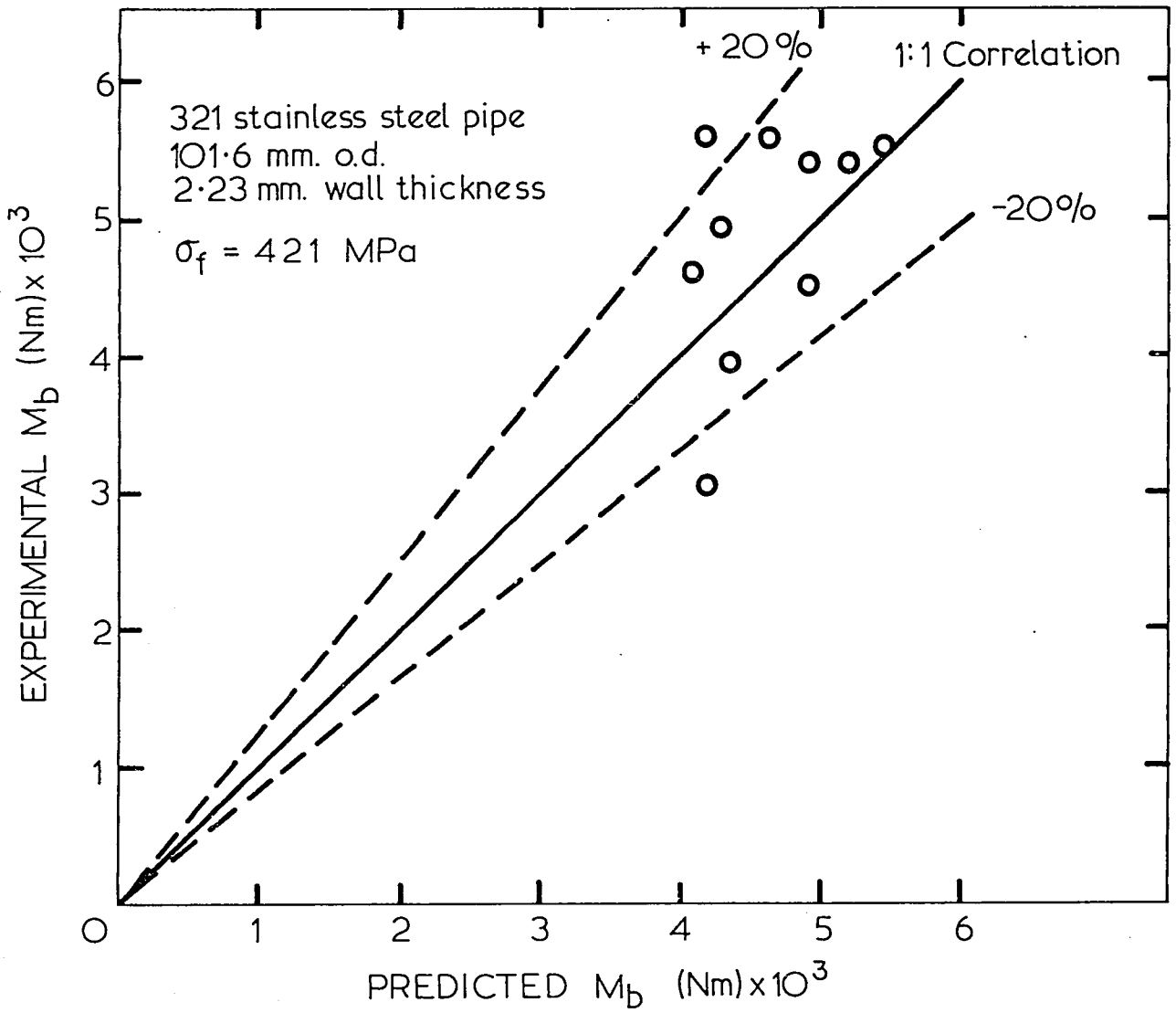


**FIGURE 6. COMPARISON OF PREDICTED AND EXPERIMENTAL RESULTS FOR THROUGH-THICKNESS FLAWS**

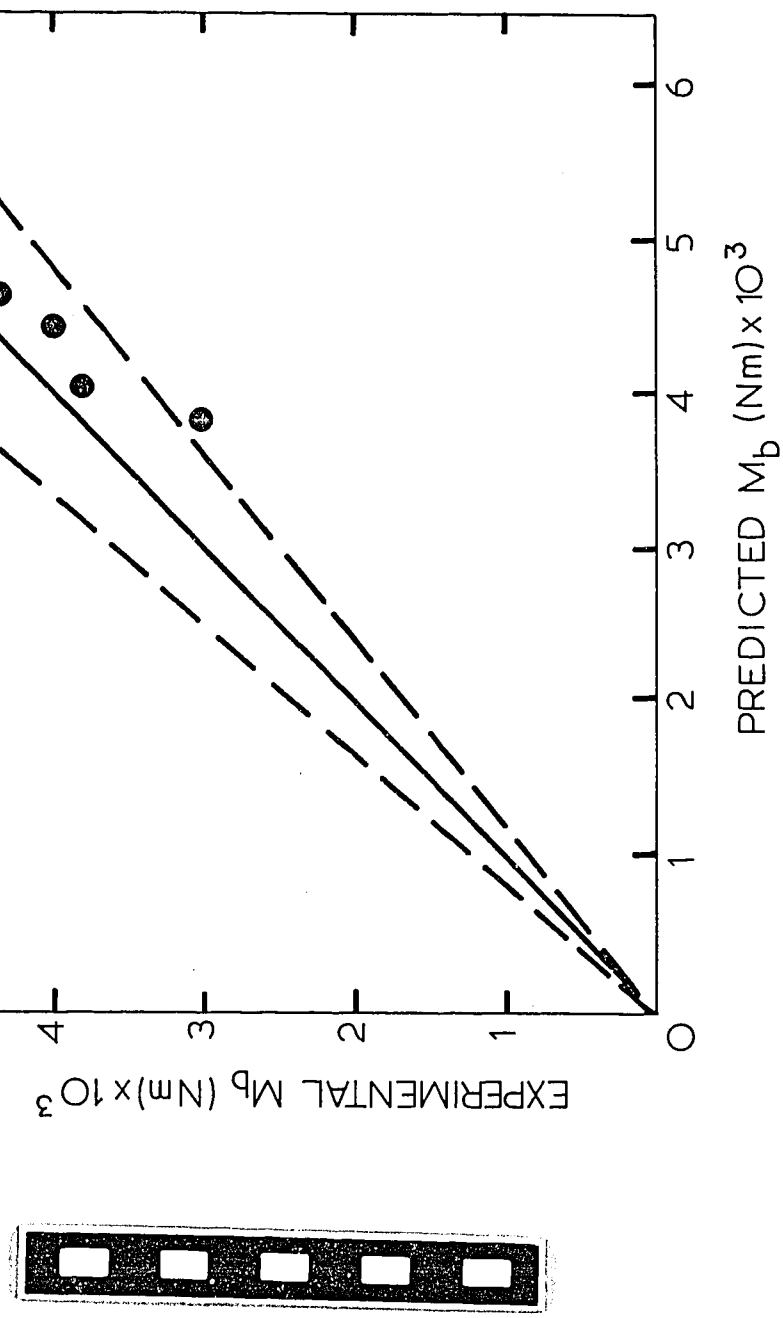


FIGURE 7. COMPARISON OF PREDICTED AND EXPERIMENTAL RESULTS FOR PARTIAL THICKNESS FLAWS